Turkish Journal of Physics

Volume 36 | Number 3 Article 15

1-1-2012

Heat and mass transfer in Hartmann flow with Soret effect in presence of a constant heat source

NAZIBUDDIN AHMED

TÜBİTAK

Turk J Phys
36 (2012) , 446 – 460.

doi:10.3906/fiz-1109-20

Heat and mass transfer in Hartmann flow with Soret effect in presence of a constant heat source

Nazibuddin AHMED
Department of Mathematics, Gauhati University, Guwahati– 781014, Assam-INDIA
e-mail: saheel_nazib@yahoo.com

Received: 04.10.2011

Abstract

An exact solution of the laminar flow of an incompressible, viscous, electrically conducting fluid between two infinite, parallel, horizontal isothermal stationary walls in the presence of a transverse magnetic field and constant heat source, taking into account the induced magnetic field, induced electric field, Soret effect and dissipating heat is presented. The expressions for the non-dimensional velocity field, temperature field, concentration field, induced magnetic field, induced electric field, skin frictions at the walls and the coefficients of the rates of heat and mass transfer at the walls in terms of the Nusselt and Sherwood numbers are obtained. The effects of the different parameters involved in the problem, namely Hartmann number, Prandtl number, Eckert number, heat source parameter, Soret number and pressure gradient on the above mentioned fields are discussed through graphs and tables. It is seen that the magnetic field has a significant effect on the flow and transport characteristics. The results obtained in this paper are consistent with the physical reality of the flow problem.

Key Words: Magnetic field, electric field, current density, induced magnetic field, viscous dissipative heat, electrically conducting, heat source, thermal diffusion

AMS Subject Classification: 76W05

1. Introduction

MHD is the science of motion of electrically conducting fluid in presence of magnetic field. Engineers apply MHD principle in fusion reactors, dispersion of metals, metallurgy, design of MHD pumps, MHD generator and MHD flow meters etc. The dynamo and motor is a classical example of MHD principle. Geophysics encounters MHD characteristics in the interaction of conducting fluid and magnetic field. MHD convection problems are also very significant in the fields of stellar and planetary magnetospheres, aeronautics and electrical engineering. The principle of MHD also finds its application in medicine and Biology. The MHD principle is also utilized in stabilizing a flow against the transition from laminar to turbulent flow.

MHD in its present form is due to the pioneer contribution of several notable authors like Alfven [1], Cowling [2], Shercliff [3], Ferraro and Plumpton [4] and Crammer and Pai [5]. The phenomenon of heat transfer

plays a significant role in many industrial and environmental problems. Industrial problems include those of production and conversion of energy and electrical power generation, minimization of the rates of heat transfer for maintaining the integrity of materials in high temperature environments, working and design of propulsion systems and cryogenics. Environmental problems include those of local and global climatology. Studies on thermal effects in buildings and other structures require applications of heat transfer principles. The study of heat transfer related problems concerning the flows of electrically conducting fluids through channels becomes very interesting and fruitful from physical point of view when a magnetic field is applied to the flow.

The first experimental and theoretical work on MHD channel flow was undertaken by Hartmann [6] and Hartmann and Lazarus [7]. Following these works [6 and 7], several other investigators have carried out model studies on MHD channel flow. Some of them are Chang and Yen [8], Sutton and Sherman [9], Soundalgekar and Bhatt [10], Badosa and Borkakati [11], Makinde and Mhone [12], Ganesh and Krishnambal [13], Chaudhary et al. [14], Anwar et al. [15] and Lahjomri et al. [16]. Recently, Ahmed and Kalita [17] have studied the problem of two dimensional steady MHD forced convective Poiseuille flow and heat transfer between two porous plates with constant pressure gradient and a heat source, taking into account the induced magnetic field.

As the present author is aware, up to now, no attempt has been made to study the problem of laminar forced convective mass transfer flow of an incompressible viscous electrically conducting fluid between two horizontal parallel isothermal stationary walls in presence of transverse magnetic field and a constant heat source, taking into account the induced magnetic field together the Soret effect. Such an attempt has been made in the present work. The thermal diffusion effect (known as Soret effect) is applied for isotope separation and in mixtures between gases with very light molecular weight like Hydrogen and Helium. The main objectives of the present work is to investigate the effect of the applied magnetic field on the velocity field, temperature field, concentration field, skin friction, Nusselt number and Sherwood number at the plates, induced magnetic field, current density and the induced electric field. It is also proposed to study the effect of dissipative heat, Prandtl number and heat source on the temperature field, concentration and on the co-efficient of the rate of heat and mass transfer from either plate to the fluid.

2. Mathematical formulations

The equations governing the steady motion of an incompressible viscous electrically conducting fluid in presence of a magnetic field and a constant heat source are: the continuity equation,

$$\vec{\nabla} \cdot \vec{q} = 0; \tag{1}$$

Gauss's law of magnetism,

$$\vec{\nabla} \cdot \vec{H} = 0; \tag{2}$$

Magnetic induction equation,

$$\vec{\nabla} \times \left(\vec{q} \times \vec{H}\right) + \eta \nabla^2 \vec{H} = 0, \tag{3}$$

where $\eta = \frac{1}{4\,\pi\,\mu_0\,\sigma}$;

Ampere's law,

$$\vec{\nabla} \times \vec{H} = 4\,\pi\,\vec{J}; \tag{4}$$

Ohm's law,

$$\vec{J} = \sigma \left[\vec{E} + \vec{q} \times \vec{B} \right]; \tag{5}$$

Momentum equation,

$$\rho \left(\vec{q}.\vec{\nabla} \right) \vec{q} = \vec{\nabla} \bar{p} + \vec{J} \times \vec{B} + \mu \nabla^2 \vec{q} + \rho \vec{g}; \tag{6}$$

Energy equation,

$$\rho C_p \left(\vec{q} \cdot \vec{\nabla} \right) \vec{q} = k \nabla^2 \bar{T} + \frac{\vec{J}^2}{\sigma} + \varphi + Q; \tag{7}$$

and the Species continuity equation,

$$\left(\vec{q} \cdot \vec{\nabla} \right) \bar{C} = D_M \nabla^2 \bar{C} + D_T \nabla^2 \bar{T}. \tag{8}$$

All of the above symbolic physical quantities are defined in the Nomenclature.

We now consider a steady laminar flow of an incompressible, viscous, electrically conducting fluid through a channel bounded by two infinite horizontal isothermal parallel plates separated by a distance $2L$ in the presence of transverse applied magnetic field $\vec{H}_0$ and a heat source. The physical model of the problem is as shown in Figure 1.

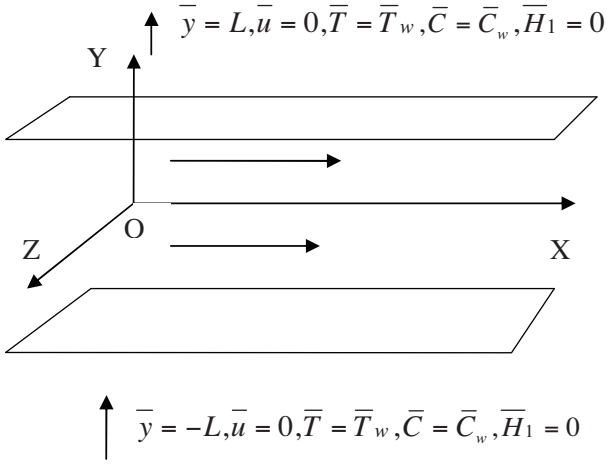

Figure 1. Physical model of the problem.

We introduce a coordinate system $(\bar{x}, \bar{y}, \bar{z})$ with the flow along the x-axis, the y-axis normal to the plates, and the z-axis along the width of the plates. Let $\vec{q} = (\bar{u}, 0, 0)$ be the fluid velocity and $\vec{H} = \left(\bar{H}_1, \bar{H}_0, 0 \right)$ be the magnetic field at point $(\bar{x}, \bar{y}, \bar{z})$ in the fluid.

Equation (1) gives

$$\frac{\partial \bar{u}}{\partial \bar{x}} = 0, \tag{9}$$

which shows that $\bar{u}$ is independent of $\bar{x}$. In the present problem $\bar{u}$ does not depend on $\bar{z}$ hence

$$\bar{u} = \bar{u}\left(\bar{y} \right). \tag{10}$$

The Gauss law of magnetism yields $\frac{\partial \bar{H}_1}{\partial \bar{x}} = 0$, which shows that

$$\bar{H}_1 = \bar{H}_1(\bar{y}). \tag{11}$$

We assume

$$\bar{p} = \bar{p}_0(\bar{x}) + \bar{p}_1(\bar{y}). \tag{12}$$

Under the assumption (12), equation (6) can be broken up to:

$$\frac{\mu_0 \bar{H}_0}{4\pi} \frac{d\bar{H}_1}{d\bar{y}} + \mu \frac{d^2\bar{u}}{d\bar{y}^2} = \frac{d\bar{p}_0}{d\bar{x}} = -\bar{P} = A \text{ constant}. \tag{13}$$

and

$$\frac{d\bar{p}_1}{d\bar{y}} + \rho\bar{g} + \frac{\mu_0}{4\pi}\bar{H}_1 \frac{d\bar{H}_1}{d\bar{y}} = 0. \tag{14}$$

Equation (3) reduces to

$$\frac{d^2\bar{H}_1}{d\bar{y}^2} + 4\pi\sigma\mu_0 \bar{H}_0 \frac{d\bar{u}}{d\bar{y}} = 0. \tag{15}$$

The energy equation (7) yields

$$\frac{k}{\rho C_p}\frac{d^2\bar{T}}{d\bar{y}^2} + \frac{\mu}{\rho C_p}\left(\frac{d\bar{u}}{d\bar{y}}\right)^2 + \frac{\sigma}{\rho C_p}\left(\bar{E} + \mu_0 \bar{u}\bar{H}_0\right)^2 + \frac{Q}{\rho C_p} = 0. \tag{16}$$

Equation (8) reduces to

$$D_M \frac{d^2\bar{C}}{d\,\bar{y}^2} + D_T \frac{d^2\bar{T}}{d\,\bar{y}^2} = 0. \tag{17}$$

Equations (4) and (5) give

$$\bar{J} = \sigma\left[E + \mu_0\,\bar{u}\,\bar{H}_0\right] = -\frac{1}{4\,\pi}\frac{d\bar{H}_1}{d\bar{y}}, \tag{18}$$

where $\bar{J} = \left|\vec{J}\right|$ and $\bar{E} = \left|\vec{E}\right|$.

We recall that there is no externally applied current for which

$$\int_{-L}^{L} \bar{J}\, d\bar{y} = 0. \tag{19}$$

The relevant boundary conditions are

$$\text{at } \bar{y} = L : \bar{u} = 0, \bar{T} = \bar{T}_w, \bar{C} = \bar{C}_w \bar{H}_1 = 0, \tag{20a}$$

$$\text{at } \bar{y} = -L : \bar{u} = 0, \bar{T} = \bar{T}_w, \bar{C} = \bar{C}_w \bar{H}_1 = 0, \tag{20b}$$

$$\text{at } \bar{y} = 0 : \bar{p}_1 = 0. \tag{20c}$$

We introduce the following non-dimensional quantities:

$$M = \mu_0 \bar{H}_0 L \sqrt{\frac{\sigma}{\mu}}, \quad y = \frac{\bar{y}}{L}, \quad x = \frac{\bar{x}}{L}, \quad z = \frac{\bar{z}}{L},$$

$$u = \frac{4\,\pi\,\sqrt{\mu\sigma}\,\bar{u}}{\bar{H}_0}, \quad h = \frac{\bar{H}_1}{\bar{H}_0}, \quad E = \frac{4\,\pi\,\bar{E}\,L\,\sigma}{\bar{H}_0}$$

$$\mathrm{Pr} = \frac{\mu C_p}{k}, \quad P = \frac{4\,\pi\,L^2\,\bar{P}\sqrt{\sigma}}{\bar{H}_0\sqrt{\mu}}, \quad g = \frac{4\,\pi\,L\rho\bar{g}}{\mu_0 \bar{H}_0^2},$$

$$J = \frac{4\,\pi\,L\,\bar{J}}{\bar{H}_0}, \quad p_0 = \frac{4\,\pi\,L\,\sqrt{\sigma}\,\bar{p}_0}{\bar{H}_0\sqrt{\mu}},$$

$$\theta = \frac{\bar{T} - \bar{T}_w}{\bar{T}_w}, \quad \mathrm{Ec} = \frac{\bar{H}_0^2}{16\,\pi^2 \mu\,\sigma\,C_p\,\bar{T}_w},$$

$$\alpha = \frac{QL^2}{\bar{T}_w\,k}, \quad Sc = \frac{\nu}{D_M}, \quad Sr = \frac{D_T \bar{T}_w}{\nu\,\bar{C}_w}, \quad p_1 = \frac{4\,\pi\,\bar{p}_1}{\mu_0 \bar{H}_0^2}, \quad \theta = \frac{\overline{C} - \overline{C}_{_w}}{\overline{C}_{_w}}$$

The non-dimensional forms of Equations (13)-(19) are as follows:

$$\frac{d^2u}{dy^2} + M\frac{dh}{dy} = -P, \tag{21}$$

$$\frac{dp_1}{dy} + g + h\frac{dh}{dy} = 0, \tag{22}$$

$$\frac{d^2h}{dy^2} + M\frac{du}{dy} = 0, \tag{23}$$

$$\frac{d^2\theta}{dy^2} + \mathrm{Pr}\,\mathrm{Ec}\left(\frac{du}{dy}\right)^2 + \mathrm{Pr}\,\mathrm{Ec}\,(E + Mu)^2 + \alpha = 0 \quad , \tag{24}$$

$$\frac{d^2\phi}{dy^2} + Sr\,Sc\frac{d^2\theta}{dy^2} = 0, \tag{25}$$

$$J = E + Mu = -\frac{dh}{dy}, \tag{26}$$

$$\int_{-1}^{1} J dy = 0. \tag{27}$$

The relevant boundary conditions are

$$\text{at } y = 1 : u = 0, \theta = 0,\ \phi = 0, h = 0, \tag{28a}$$

$$\text{at } y = -1 : u = 0, \theta = 0,\ \phi = 0 h = 0, \tag{28b}$$

$$\text{at } y = 0, p_1 = 0. \tag{28c}$$

The solution of the equation (22) subject to the boundary condition (28c) is

$$p_1 + gy + \frac{h^2}{2} = 0. \tag{29}$$

The equation (23) yields

$$\frac{dh}{dy} + Mu = C_2, \tag{30}$$

C_2 being a constant. The equation (26) gives

$$E = -\left(\frac{dh}{dy} + Mu\right) = -C_2. \tag{31}$$

Equations (30) and (31) yield

$$\frac{dh}{dy} + Mu = -E. \tag{32}$$

Equations (21) and (32) together give

$$\frac{d^2u}{dy^2} - M^2u = ME - P. \tag{33}$$

The solution of equation (33), subject to boundary conditions (28a) and (28b), is

$$u = \begin{cases} \frac{P-ME}{M^2}\left[1 - \frac{Cosh(My)}{CoshM}\right] & \text{for} \quad M \neq 0, \\ \frac{P}{2}\left(1 - y^2\right) & \text{for} \quad M = 0. \end{cases} \tag{34}$$

Equations (26) and (27) give

$$E = \begin{cases} \frac{P}{M}\left(1 - M\,CothM\right) & \text{for} \quad M \neq 0 \\ 0 & \text{for} \quad M = 0 \end{cases} \tag{35}$$

Equations (32), (34) and (35) subsequently yield

$$h = \begin{cases} \frac{P}{M}\left[\frac{Sinh(My)}{SinhM} - y\right] & \text{for} \quad M \neq 0, \\ 0 & \text{for} \quad M = 0. \end{cases} \tag{36}$$

The equation (26) gives

$$J = \begin{cases} \frac{P}{M}\left[1 - \frac{M\cosh My}{SinhM}\right] & \text{for} \quad M \neq 0, \\ 0 & \text{for} \quad M = 0. \end{cases} \tag{37}$$

The solutions of the equation (24) subject to the boundary conditions (28a) and (28b) are

$$\begin{aligned} \theta \quad = \quad & \tfrac{A_0}{2}\left(1 - y^2\right) + \tfrac{A_1}{M^2}\left(CoshM - CoshMy\right) \\ & + \tfrac{A_2}{4M^2}\left[Cosh\left(2M\right) - Cosh\left(2My\right)\right], M \neq 0, \end{aligned} \tag{38}$$

and

$$\theta = \frac{\alpha}{2}\left(1 - y^2\right) + \frac{\mathrm{Pr\,Ec}}{12}\left(1 - y^4\right), \quad M = 0, \tag{39}$$

where

$$A_0 = \alpha + \Pr \mathrm{Ec} B^2, \quad A_1 = -\frac{2 \Pr \mathrm{Ec} AB}{Cosh M},$$
$$A_2 = -\frac{\Pr \mathrm{Ec} A^2}{Cosh^2 M}, \quad B = E + A, \quad A = \frac{P - ME}{M}.$$

Equation (25) gives

$$\phi = -Sr\, Sc\, \theta. \tag{40}$$

3. Co-efficient of skin friction

The shear stress at any point in fluid is given by

$$\bar{\tau} = \mu \frac{d\bar{u}}{d\bar{y}} = \frac{\bar{H}_0}{4\pi L} \sqrt{\frac{\mu}{\sigma}} \frac{du}{dy} = \tau_0 \frac{du}{dy}, \tau_0 = \frac{\bar{H}_0}{4\pi L} \sqrt{\frac{\mu}{\sigma}}. \tag{41}$$

The co-efficient of skin friction at any point is given by the relation

$$\tau = \frac{\bar{\tau}}{\tau_0} = \frac{du}{dy}. \tag{42}$$

The co-efficient of skin frictions at the walls $y = 1$ and $y = -1$ are, respectively, given by the relations

$$\tau_1 = \frac{du}{dy}\Big]_{y=1} = \begin{cases} \frac{ME-P}{M} \tanh M & \text{for} \quad M \neq 0, \\ -P & \text{for} \quad M = 0, \end{cases} \tag{43}$$

and

$$\tau_2 = \frac{du}{dy}\Big]_{y=-1} = \begin{cases} \frac{P-ME}{M} \tanh M & \text{for} \quad M \neq 0, \\ P & \text{for} \quad M = 0. \end{cases} \tag{44}$$

4. Rate of heat transfer

The co-efficient of the rate of heat transfer at any point in fluid in terms of Nusselt number Nu is given by

$$Nu = -\frac{L}{\bar{T}_w} \frac{d\bar{T}}{d\bar{y}} = -\frac{d\theta}{dy} \tag{45}$$

The Nusselt numbers at the walls $y = 1$ and $y = -1$ are as follows:

$$Nu_1 = -\frac{d\theta}{dy}\Big]_{y=1} = \begin{cases} A_0 + \frac{A_1}{M} Sinh M + \frac{A_2}{2M} Sinh\,(2M) & \text{for} \quad M \neq 0, \\ \alpha + \frac{\Pr \mathrm{Ec} P^2}{3} & \text{for} \quad M = 0, \end{cases} \tag{46}$$

$$Nu_2 = -\frac{d\theta}{dy}\Big]_{y=-1} = \begin{cases} -A_0 - \frac{A_1}{M} Sinh M - \frac{A_2}{2M} Sinh\,(2M) & \text{for} \quad M \neq 0, \\ -\alpha - \frac{\Pr \mathrm{Ec} P^2}{3} & \text{for} \quad M = 0. \end{cases} \tag{47}$$

5. Rate of mass transfer

The coefficient of the rate of mass transfer at any point in fluid in terms of Sherwood number Sh is given by

$$Sh = -\frac{L}{\bar{C}_w}\frac{d\bar{C}}{d\bar{y}} = -\frac{d\phi}{dy} \tag{48}$$

The Sherwood numbers at the walls $y = 1$ and $y = -1$ are respectively given by the relations

$$Sh_1 = -\left.\frac{d\phi}{dy}\right]_{y=1} = Sr\,Sc\left.\frac{d\theta}{dy}\right]_{y=1} = -Sr\,ScNu_1, \tag{49}$$

$$Sh_2 = -\left.\frac{d\phi}{dy}\right]_{y=-1} = Sr\,Sc\left.\frac{d\theta}{dy}\right]_{y=-1} = -Sr\,ScNu_2. \tag{50}$$

6. Results and Discussion

In order to get physical insight into the problem, we have carried out numerical calculations for the non dimensional velocity u, induced magnetic field h, current density J, temperature θ and the Nusselt numbers Nu_1 and Nu_2 at the plates $y = 1$ and $y = -1$ and the coefficient of skin friction τ_1 and τ_2 at these plates, by assigning some selected values to the parameters entering into the problem and the effect of these values are demonstrated through different graphs and tables.

Figure 2 and Figure 3 show the variation of the velocity field u versus y under the influence of the Hartmann number M and the pressure gradient P. These two figures clearly establish the fact that the fluid motion is retarded due to imposition of the transverse magnetic field and accelerated under the pressure gradient. This phenomenon clearly agrees with the physical reality. These figures further indicate that the velocity increases sharply in a thin layer adjacent to either plate and there after it slightly decreases and remains almost stationary in the central portion of the channel.

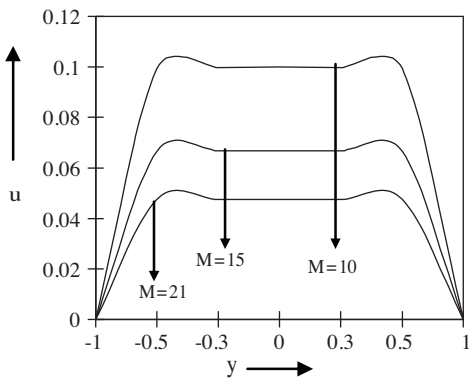

Figure 2. Velocity u versus y for $P = 1$ Ec $= 0.4$, Pr $= 7$ and $\alpha = 0.8$.

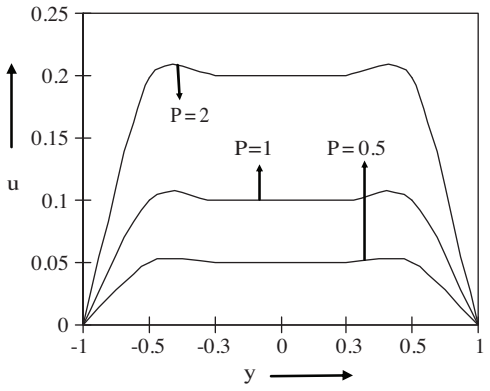

Figure 3. Velocity u versus y for $M = 10$, Ec $= 0.4$, Pr $= 7$ and $\alpha = 0.8$.

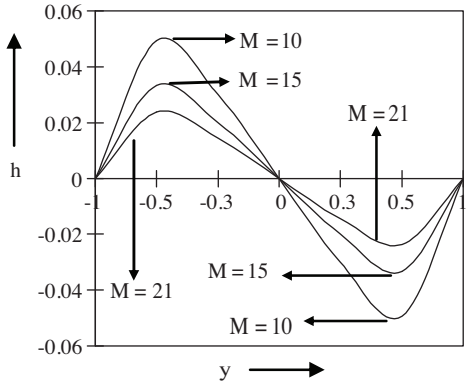

Figure 4. Induced magnetic field h versus y for $P = 1$, Ec $= 0.4$, Pr $= 7$ and $\alpha = 0.8$.

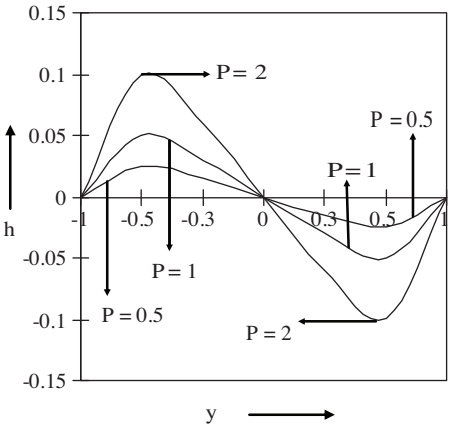

Figure 5. Induced magnetic field versus y for $M = 10$, Ec $= 0.4$, Pr $= 7$ and $\alpha = 0.8$.

It is observed from Figures 4 and 5 that the pressure gradient causes the induced magnetic field to increase whereas an increase in the magnetic parameter M results in a steady fall of the induced magnetic field.

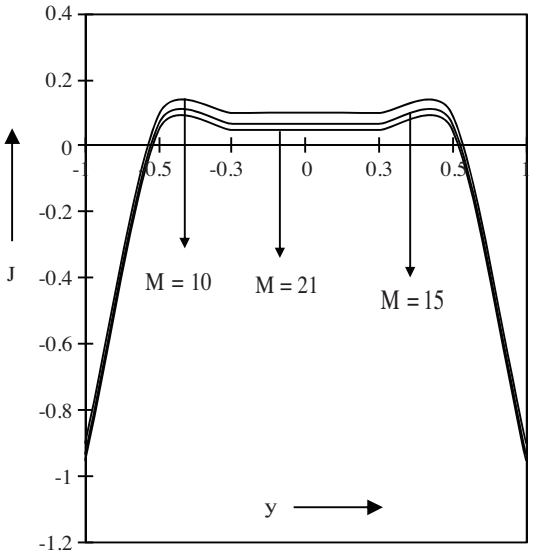

Figure 6. Current Density J, versus y for $P = 1$, Ec $=$ 0.4, Pr $= 7$ and $\alpha = 0.8$.

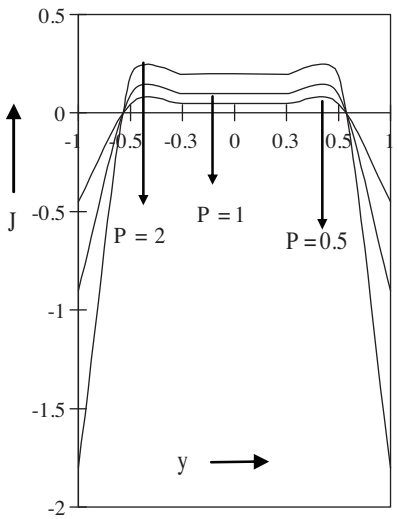

Figure 7. Current Density J, versus for M=10, Ec=0.4, Pr=7 and $\alpha = 0.8$ and $\alpha = 0.8$.

Figures 6 and 7 show the change of behavior of the current density J against y under M and P. Like velocity, here we also notice that the current density rises up under the pressure gradient and falls down for increasing Hartmann number. Moreover it rises sharply near the plates and remains uniform in the central portion of the channel.

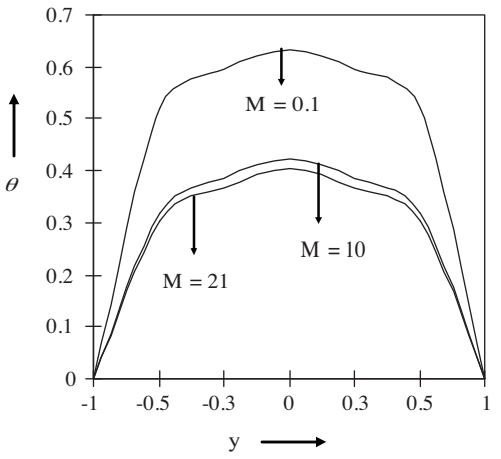

Figure 8. Temperature θ versus y for $P = 1$, Pr = 7, Ec = 0.4 and $\alpha = 0.8$.

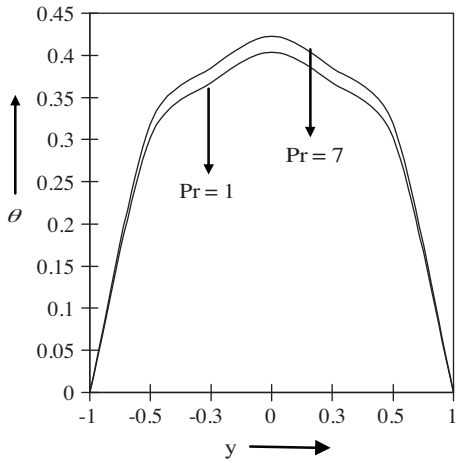

Figure 9. Temperature θ versus y for $P = 1$, $M = 10$, Ec = 0.4 and $\alpha = 0.8$.

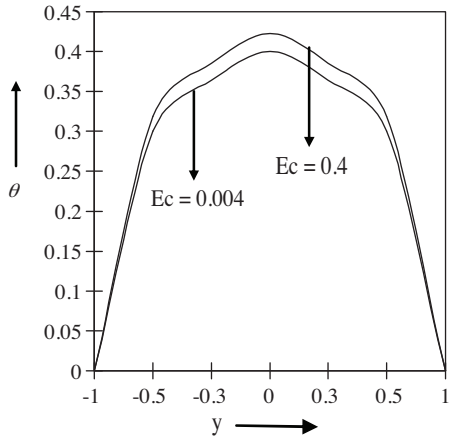

Figure 10. Temperature θ versus y for $P = 1$, $M = 10$, Pr = 7 and $\alpha = 0.8$.

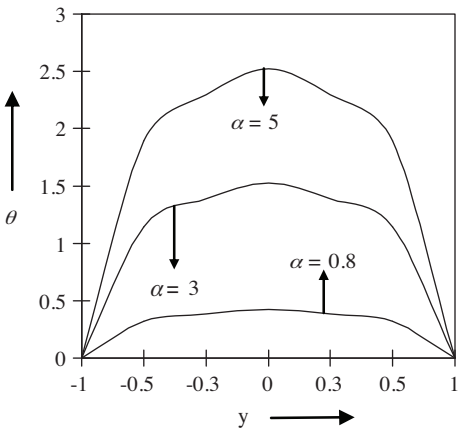

Figure 11. Temperature θ versus y For $P = 1$, $M = 10$, Pr = 7 and Ec = 0.4.

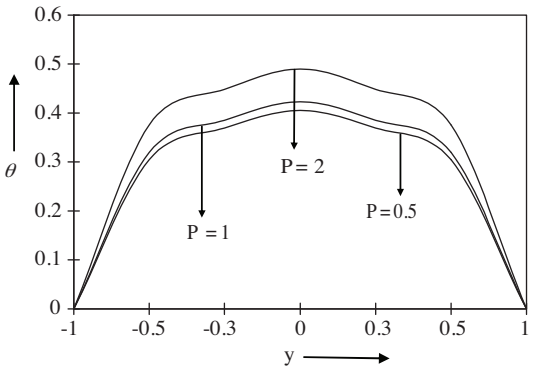

Figure 12. Temperature θ versus y for $M = 10$, Ec = 0.4, Pr = 7 and $\alpha = 0.8$.

The variation of the temperature field θ as a function of y under the effect of the Hartmann number

M, the Prandtl number Pr, the Eckert number Ec, the heat source parameter α and the pressure gradient P is demonstrated in Figures 8–12. These figures show that the fluid temperature falls due to imposition of the transverse magnetic field, but it rises due to dissipative heat, heat generation source and pressure gradient. This phenomenon has good agreement with the laws of physics.

Equation (40) shows that the concentration distribution is proportional to the temperature distribution as their magnitudes are concerned. The same phenomena holds well for the local coefficients of heat and mass transfer also, as seen in equations (49) and (50). The temperature profiles show that $\theta \geq 0 \ \forall -1 \leq y \leq 1$. That is, $\bar{T} \geq \bar{T}_w$ in the fluid region, which indicates that the heat flux occurs from the fluid to either plate. On the other hand, equation (40) yields that $\phi \leq 0 \ \forall \ -1 \leq y \leq 1$ which implies that $\bar{C} \leq \bar{C}_w$ in the entire channel, and it causes that the mass is transferred from the walls to the fluid. Equations (40), (49) and (50) establish the fact that the magnitude of the fluid concentration as well as the local co-efficient of the rate of mass transfer (Sherwood number) linearly depends on Sr or Sc. In other words, the magnitude of the fluid concentration rises under the thermal diffusion effect and falls due to mass diffusion.

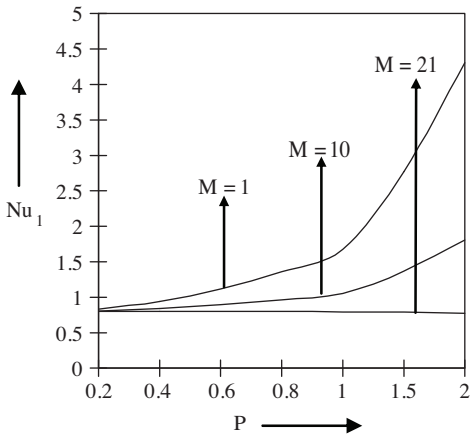

Figure 13. Nusselt number Nu_1 versus P for Pr =7, Ec = 0.4 and $\alpha = 0.8$.

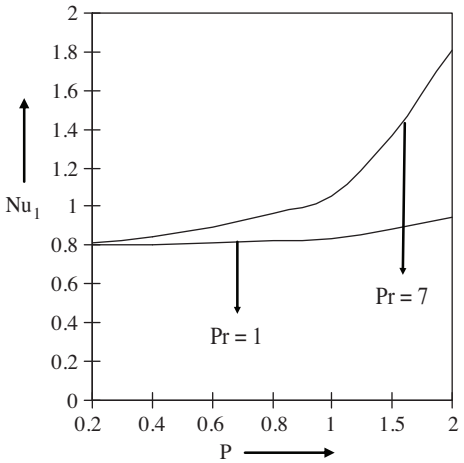

Figure 14. Nusselt number Nu_1 versus P for M = 10, Ec = 0.4 and $\alpha = 0.8$

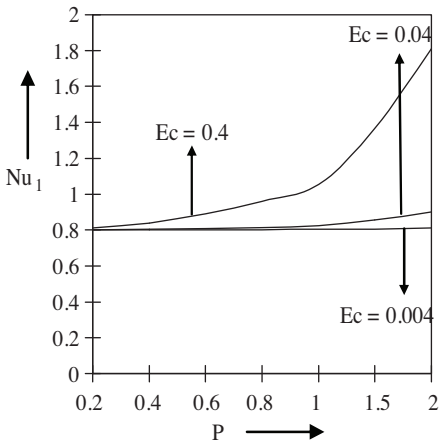

Figure 15. Nusselt number Nu_1 versus P for $M = 10$, Pr = 7 and $\alpha = 0.8$.

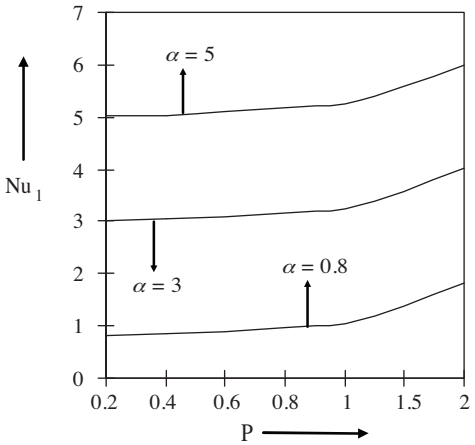

Figure 16. Nusselt number Nu_1 versus P for M = 10, Pr = 7 and Ec = 0.4.

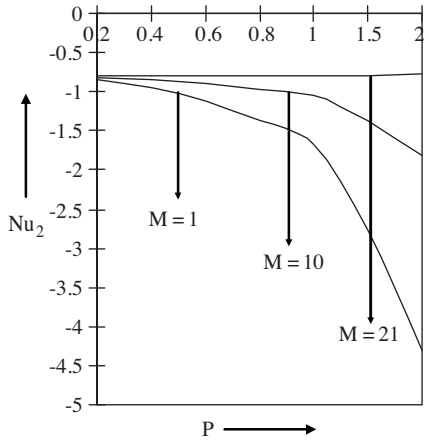

Figure 17. Nusselt number Nu_2 versus P for Pr = 7, Ec = 0.4 and $\alpha = 0.8$.

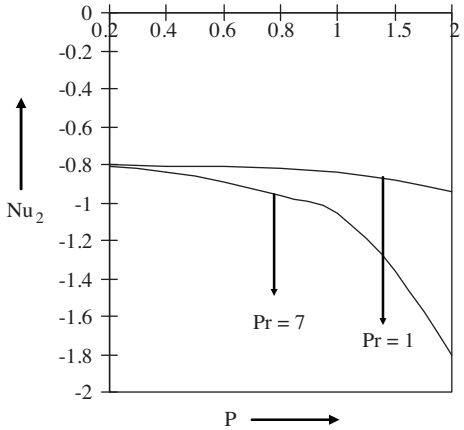

Figure 18. Nusselt number Nu_2 versus P for $M = 10$, Ec = 0.4 and $\alpha = 0.8$.

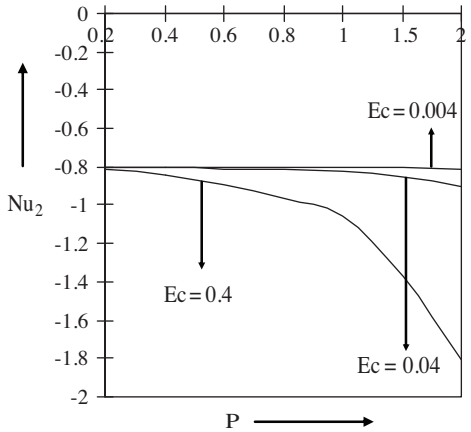

Figure 19. Nusselt number Nu_2 versus P for M = 10, Pr = 7 and $\alpha = 0.8$.

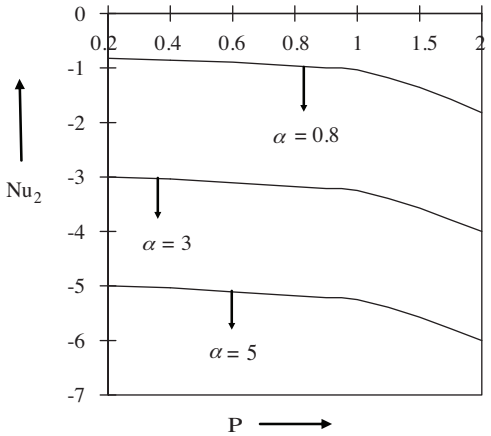

Figure 20. Nusselt number Nu_2 versus P for $M = 10$, Pr = 7 and Ec = 0.4.

Figures 13–20 show how the behavior of the coefficient of the rate of heat transfer from either plate to the fluid is affected under influence of parameters M, P, Pr, Ec and α. We observe here that the rate of heat transfer from either plate to the fluid increases under the effect of the parameters, P, Pr, Ec and α, but falls under the effect of M. That is, the application of the pressure gradient, the presence of dissipative heat as well as heat generation source and Prandtl number result in a rise of the rate of heat transfer from plate to the fluid, although the application of the transverse magnetic field causes it to fall.

From Figure 21, it is noted that the dimensionless concentration field θ increases in magnitude as the Soret number Sr increases. This behavior is observed in the fluid region bounded in between the two walls. The Soret effect is marked in the middle of the channel and is least at the walls.

Figures 22 and 23 indicate that a rise in Soret number Sr leads to a corresponding rise in the magnitudes of mass flux namely $|Sh_1|$ and $|Sh_2|$ at the upper and lower walls respectively. It is seen that as P increases, $|Sh_1|$ decreases and $|Sh_2|$ increases.

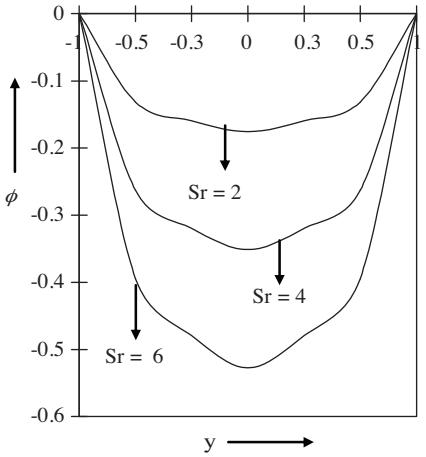

Figure 21. Concentration φ versus y for $P = 1$, $M = 10$, Pr $= 0.71$, Ec $= 0.4$, $Sc = 0.22$ and $\alpha = 0.8$.

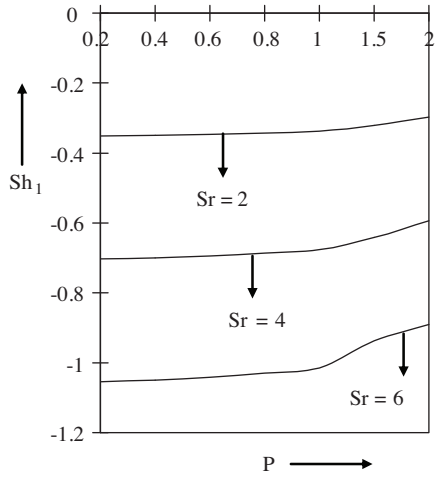

Figure 22. Sherwood number Sh_1 versus P for $M = 10$, Pr $= 0.71, Sc = 0.22$, Ec=0.4 and $\alpha = 0.8$.

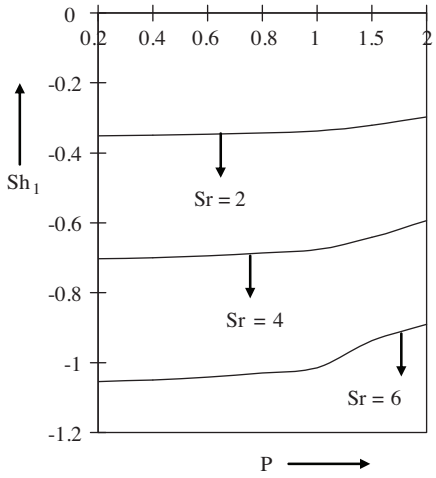

Figure 23. Sherwood number Sh_2 versus P for $M = 10$, Pr $= 0.71, Sc = 0.22$, Ec=0.4 and $\alpha = 0.8$.

Tables 1 and 2 indicate that the viscous drag at either plate is reduced when the strength of the magnetic is increased or the pressure gradient is decreased.

Table 1. Shear stress τ_1 against M, versus P for $\alpha = 0.8$ and Ec $= 0.4$.

P	τ_1 (M = 10)	τ_1 (M = 21)
0.2	-0.2000	-0.1999
0.4	-0.4000	-0.3999
0.6	-0.6000	-0.5999
0.8	-0.8000	-0.7999
1	-1.0000	-0.9999
1.5	-1.5000	-1.4999
2	-2.0000	-1.9999

Table 2. Shear stress τ_2 against M, versus P for $\alpha = 0.8$ and Ec $= 0.4$.

P	τ_2 (M = 10)	τ_2 (M = 21)
0.2	0.2000	0.1999
0.4	0.4000	0.3999
0.6	0.6000	0.5999
0.8	0.8000	0.7999
1	1.0000	0.9999
1.5	1.5000	1.4999
2	2.0000	1.9999

7. Conclusions

Our investigation leads to the following conclusions.

1. The fluid motion is retarded due to imposition of the transverse magnetic field and accelerated under the pressure gradient.
2. The pressure gradient causes the induced magnetic field to increase, whereas an increase in the magnetic parameter M results in a steady fall of the induced magnetic field.
3. The fluid temperature falls due to imposition of the transverse magnetic field, but it rises due to dissipative heat, heat generation source and pressure gradient.
4. The pressure gradient, the presence of dissipative heat as well as heat generation source and Prandtl number result in a rise of the rate of heat transfer from plate to the fluid whereas a reverse effect is observed under the magnetic field effect.
5. The viscous drag at either plate is reduced when the strength of the magnetic is increased or the pressure gradient is decreased.
6. The concentration distribution is proportional to the temperature distribution as their magnitudes are concerned. The same phenomena hold good for the local coefficients of heat and mass transfer also.
7. The magnitude of the fluid concentration rises under the thermal diffusion effect and falls due to mass diffusion.
8. The Soret effect raises the magnitude of the species concentration field. The Soret effect (thermal diffusion) on the concentration field is striking in the middle of the channel and is least at the walls.
9. The pressure gradient causes the magnitude of mass flux at the upper wall to decrease and the magnitude of mass flux at the lower wall to increase. The Soret effect (thermal diffusion) raises the magnitudes of mass flux at the walls of the channel.

Nomenclature

$\vec{B}$	Magnetic induction vector	Pr	Prandtl number
$\bar{C}$	Species concentration	$\overline{P}$	Pressure gradient
C_p	Specific heat at constant pressure	P	Dimensionless pressure gradient
D_M	Molecular mass diffusivity	p_0	Dimensionless mean pressure
D_T	Thermal diffusivity (Chemical)	p_1	Dimensionless perturbed pressure
$\vec{E}$	Electric field vector	Q	Constant heat source
E	Dimensionless electric field	$\vec{q}$	Velocity vector
$\bar{E}$	Dimensional electric field	Sc	Schmidt number
Ec	Eckert number	Sr	Soret number
$\vec{g}$	Acceleration due to gravity	$\bar{T}$	Temperature
g	Dimensionless acceleration due to gravity	$\bar{T}_w$	Temperature at either plate
$\bar{H}_0$	Intensity of the applied magnetic field	$\bar{u}$	$\bar{x}-$Component of the fluid velocity
$\vec{H}$	Magnetic field intensity vector	$(\bar{x}, \bar{y}, \bar{z})$	Cartesian coordinates
$\vec{H}_1$	Induced magnetic field vector	(x, y, z)	Dimensionless coordinates

$\bar{H}_1$	Dimensional induced magnetic field	η	Magnetic diffusivity
h	Dimensionless induced magnetic field	μ_0	Magnetic permeability
$\hat{i}, \hat{j}, \hat{k}$	Unit vectors along the co-ordinate axes	σ	Electrical conductivity
$\vec{J}$	Current density vector	ρ	Fluid density
J	Dimensionless current density	μ	Co-efficient of viscosity
$\overline{J}$	Dimensional current density	κ	Thermal conductivity fluid
L	Half of the distance between the parallel walls.	φ	Dissipation of energy due to viscosity
M	Hartmann number	θ	Dimensionless temperature
$\bar{p}$	Fluid pressure	ϕ	Dimensionless concentration
$\bar{p}_0(x)$	Mean pressure	α	Dimensionless heat source
$\bar{p}_1(y)$	Perturbed pressure		

Acknowledgement

The authors are thankful to UGC for supporting this research work under MRP (F. No. 36-96/2008(SR))

References

[1] H. Alfven, *Nature.*, **150**, (1942), 405.

[2] T .G. Cowling, Magneto hydrodynamics, Wiley Inter Science, (New York. 1957).

[3] J. A. Shercliff, A text book of Magneto hydrodynamics, (Pergamon Press, London. 1965).

[4] V. C. A. Ferraro and C. Plumpton, An introduction to Magneto Fluid Mechanics, (Clarandon Press, Oxford. 1966).

[5] K. P. Crammer and S. L. Pai, Magneto-fluid Dynamics for Engineers and applied Physics, (Mc-Graw Hill book Co. New York. 1978).

[6] J. Hartmann, *K.Dan. Vidensk.Selsk. Mat. Fys. Medd.*, **15**, (1937), 1.

[7] J. Hartmann and Lazarus, *K.Dan. Vidensk.Selsk. Mat. Fys. Medd.*, **15**, (1937), 1.

[8] C.C . Chang and J. T. Yen, *Phys. Fluids,* **4**, (1961), 1355.

[9] G. W. Sutton and A. Sherman, Engineering Magneto hydrodynamics, (McGraw-Hill Book Co., Inc., New York. 1965).

[10] V. M. Soundalgekar and J. P. Bhatt, Oscillatory MHD channel flow and heat transfer, *Indian J. Pure Appl. Math.,* **15**, (1984), 819.

[11] G. Bodosa and A. K. Borkakati, *Indian Jour. of Theo. Phys.*, **51**, (2003), 39.

[12] O. D. Makinde and P.Y. Mhone, *Rom. Jour. Phys.*, **50**, (2005), 931.

[13] S. Ganesh and S. Krishnambal, *Journal of Applied Sciences*, **6**, (2006), 2420.

[14] R. C. Chaudhary, A. K. Jha and S. S. Dhayal, *J. Rajasthan Acad. Phy. Sci.,* **5**, (2006), 233.

[15] O. Anwar, B. J. Zuecob and H. S. Takhar, *Communications in Nonlinear Science and Numerical Simulation*, **14**, (2009), 1082.

[16] J. Lahjomri, A. Oubarra and A. Alemany, *International Journal of Heat and Mass Transfer*, **45,** (2002), 1127.

[17] N. Ahmed and D. Kalita, *Bull. Cal. Math. Soc.*, **102**, (2010), 107.